

Climate impacts of geoengineering marine stratocumulus clouds

Andy Jones,¹ Jim Haywood,¹ and Olivier Boucher¹

Received 11 November 2008; revised 27 February 2009; accepted 16 March 2009; published 27 May 2009.

[1] Theoretical potential geoengineering solutions to the global warming problem have recently been proposed. Here, we present an idealized study of the climate response to deliberately seeding large-scale stratocumulus cloud decks in the North Pacific, South Pacific, and South Atlantic, thereby inducing cooling via aerosol indirect effects. Atmosphere-only, atmosphere/mixed-layer ocean, and fully coupled atmosphere/ocean versions of the Met Office Hadley Centre model are used to investigate the radiative forcing, climate efficacy, and regional response of temperature, precipitation, and net primary productivity to such geoengineering. The radiative forcing simulations indicate that, for our parameterization of aerosol indirect effects, up to 35% of the radiative forcing due to current levels of greenhouse gases could be offset by stratocumulus modification. Equilibrium simulations with the atmosphere/mixed-layer ocean model, wherein each of the three stratocumulus sheets is modified in turn, reveal that the most efficient cooling per unit radiative forcing occurs when the South Pacific stratocumulus sheet is modified. Transient coupled model simulations suggest that geoengineering all three stratocumulus areas delays the simulated global warming by about 25 years. These simulations also indicate that, while some areas experience increases in precipitation and net primary productivity, sharp decreases are simulated in South America, with particularly detrimental impacts on the Amazon rain forest. These results show that, while some areas benefit from geoengineering, there are significant areas where the response could be very detrimental with implications for the practical applicability of such a scheme.

Citation: Jones, A., J. Haywood, and O. Boucher (2009), Climate impacts of geoengineering marine stratocumulus clouds, *J. Geophys. Res.*, 114, D10106, doi:10.1029/2008JD011450.

1. Introduction

[2] Anthropogenic emissions of carbon dioxide from fossil fuel burning are widely accepted as the primary cause of global warming, and the rate of temperature change is projected to increase in the future in the absence of climate change mitigation policy [IPCC, 2007]. Many geoengineering solutions have been proposed in order to counteract global warming [Morton, 2007; Boyd, 2008]. These geoengineering proposals fall into two categories: those attempting to capture carbon dioxide from the atmosphere via technological or biological sequestration [e.g., Lackner, 2003], and those attempting to reflect some of the sun's radiation so as to counterbalance the warming from greenhouse gases with a deliberate geoengineered cooling. Various methods have been suggested for increasing the albedo of the planet and inducing such a cooling [e.g., Angel, 2006; Bower et al., 2006; Crutzen, 2006; Wigley, 2006]. One such suggestion [Latham, 1990, 2002; Bower et al., 2006; Latham et al., 2008] is to increase the albedo of low-level marine clouds by injecting large amounts of sea salt aerosol into the marine boundary layer in certain regions using a fleet of cloud seeding ships [Salter et al., 2008]. The suggestion is that

the sea salt aerosol would act as cloud condensation nuclei and so increase the reflectivity of the modified cloud via the first (albedo) and second (precipitation efficiency) indirect effects [Twomey, 1977; Albrecht, 1989]. Such clouds, being low level, act to cool the climate system, and the suggestion is that modifying them would enhance this cooling.

[3] Here we do not attempt to address issues regarding the plausibility and detailed aerosol-cloud microphysical aspects of this geoengineering proposal, nor the implications of such geoengineering solutions in political or ethical contexts [see Robock, 2008]. Instead, we attempt to assess the climate impact of such a scheme within a state-of-the-art climate model. We assume that the proposed method works as envisioned by its proponents: that increasing sea salt aerosol concentration in extensive areas of low-level marine cloud, which in turn decreases cloud droplet effective radius, increases cloud albedo, cloud lifetime and areal extent. We assess the radiative forcing produced by such changes in different parts of the world, and how these changes then affect global and regional temperature and precipitation patterns and determine the effect on net primary productivity over land.

2. Experimental Description

[4] The model used in this study is a version of the Hadley Centre Global Environment Model version 2,

¹Met Office Hadley Centre, Exeter, UK.

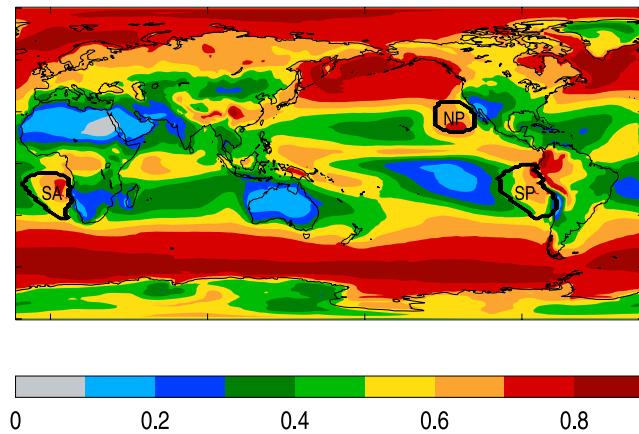


Figure 1. Location and extent of the three regions of persistent marine stratocumulus clouds identified in ISCCP data that are considered in this study. North Pacific (NP), South Pacific (SP), and South Atlantic (SA) plotted over the total cloud fraction from the control simulation of HadGEM2-AML (see section 3.2).

HadGEM2 [Collins *et al.*, 2008], which is an updated version of the HadGEM1 model [Johns *et al.*, 2006] and includes the same treatment of atmospheric radiation and clouds. The treatment of aerosols and their direct and indirect effects in this model are described by Jones *et al.* [2001], Bellouin *et al.* [2007], and Jones *et al.* [2007]. The model also includes the MOSES-2 land surface scheme [Essery *et al.*, 2003] which includes a treatment of the carbon exchange with vegetation. Three different configurations of the model were used:

[5] 1. HadGEM2-A: an atmosphere-only configuration which is used for obtaining approximate estimates of the radiative forcing caused by the cloud modification;

[6] 2. HadGEM2-AML: a configuration where the atmosphere is coupled to a mixed-layer ocean model to determine the sensitivity of climate to cloud modification in different regions;

[7] 3. HadGEM2-AO: a configuration where the atmosphere is coupled to a fully dynamical ocean to determine the temporal and spatial patterns of the climate response.

[8] Various geographical distributions of cloud modification might be considered [e.g., Latham *et al.*, 2008], but here we consider the modification of geographically extensive marine stratocumulus cloud sheets as considered by Bower *et al.* [2006]. Such persistent cloud regimes are deemed the best all-year targets for geoengineering [Salter *et al.*, 2008] as they have a high fraction of low-level cloud with little overlying high-level cloud, and generally have fairly low cloud droplet number concentration (CDNC) values, making them susceptible to modification by the addition of sea salt aerosols. Moreover, being located near continents, these stratocumulus cloud sheets are readily accessible, which would facilitate deployment and maintenance of the cloud seeding ships. The extent and location of regions of climatologically significant marine stratocumulus clouds were estimated from distributions of low-level clouds of intermediate optical thickness (between 3.6 and 23 at visible wavelengths) as categorized by the Interna-

tional Satellite Cloud Climatology Project (ISCCP [Rossow and Schiffer, 1999]). Three main regions of persistent marine stratocumulus were identified in the ISCCP data, on the eastern sides of the North Pacific (NP), South Pacific (SP) and South Atlantic (SA), as shown in Figure 1.

[9] As mentioned in the Introduction, we made no attempt to model the aerosol, dynamical or cloud microphysical processes involved in injecting sea salt aerosol into low-level marine clouds. Instead, the process was assumed to work as envisaged, and boundary layer CDNC values in the regions to be modified were set to the asymptotic maximum in the model (375 cm^{-3} [Jones *et al.*, 2001]). This compares with mean unperturbed stratocumulus CDNC values in the model of around 100 cm^{-3} , ranging from greater than 300 cm^{-3} near the coasts to below 50 cm^{-3} at the westward extent of the regions that are modified. Note that the CDNC changes do not propagate outside the modified region; any changes induced outside these regions are driven by dynamical feedbacks in response to the applied perturbation. The simulations can be envisaged as an idealized deployment of a fully functioning fleet of geoengineering vessels [see Salter *et al.*, 2008] that all become operational at the same time in the specific locations described below.

[10] Three sets of experiments were performed. The first set were atmosphere-only simulations using HadGEM2-A to evaluate the radiative forcing produced by modifying in turn the CDNC in each of the stratocumulus decks identified above (NP, SP and SA), as well as when all three were modified simultaneously (ALL). A control simulation with no cloud modification was also performed. The simulations were run for 10 years under conditions appropriate for the year 2000, and the mean difference in top-of-atmosphere net radiation between each experiment and the control simulation was taken as a measure of the forcing. As the meteorology is different in the control and experiment simulations, this is not a true forcing as defined by IPCC [2007], and will be referred to as the radiative flux perturbation (RFP [Haywood *et al.*, 2009]). The advantage of this method over the strictly defined forcing by IPCC [2007] is that it allows the radiative impact of aerosols on both cloud albedo and precipitation efficiency to be evaluated.

[11] A second set of experiments was performed with the atmosphere/mixed-layer model to investigate the relative climate sensitivity to modifying the various stratocumulus cloud areas. These experiments (in Control, NP, SP, SA and ALL configurations) were run for 30 years using greenhouse gas concentrations and aerosol emissions appropriate for the year 2000. The results presented are means of the final 20 years, after the simulations had reached equilibrium.

[12] Finally, a third set of experiments was performed with the fully coupled atmosphere-ocean model to investigate the climate impact of the geoengineering. A simulation run in permanent “1860” conditions was used to spin up the atmosphere-ocean system and to provide a baseline against which to assess climate change in the other simulations. A transient simulation was then initialized from this experiment and run from 1860 to 2000 using historical changes in atmospheric constituents, aerosol emissions and land use. This simulation was then continued from 2000 to 2060 using the A1B scenario from the IPCC Special Report on

Table 1. Annual Mean Radiative Flux Perturbation Caused by Modifying CDNC in Various Stratocumulus Regions (W m^{-2} , $\pm 1\text{SD}$)^a

Area Modified	Global	NH	SH	Sc	RoW	Area (%)
NP	-0.45 ± 0.08	-0.70 ± 0.11	-0.19 ± 0.08	-0.26 ± 0.01	-0.18 ± 0.08	0.7
SP	-0.52 ± 0.09	-0.04 ± 0.15	-1.00 ± 0.08	-0.45 ± 0.01	-0.07 ± 0.09	1.5
SA	-0.34 ± 0.09	$+0.02 \pm 0.14$	-0.71 ± 0.09	-0.34 ± 0.01	-0.003 ± 0.09	1.1
ALL	-0.97 ± 0.09	-0.32 ± 0.16	-1.62 ± 0.06	-1.06 ± 0.02	$+0.09 \pm 0.09$	3.3

^aVarious regions: global, northern hemisphere (NH), southern hemisphere (SH), RFP due to modified cloud areas (Sc) and unmodified rest-of-world (RoW), and the area of the modified cloud regions (% of Earth's surface area).

Emission Scenarios (SRES [Nakićenović *et al.*, 2000]) to act as a control. The geoengineering simulations (configurations NP, SP, SA and ALL) were initialized at 2000 and run to 2060 under the A1B scenario but also modifying CDNC in the appropriate stratocumulus areas.

3. Results

3.1. Radiative Flux Perturbations

[13] The RFP (“forcing”) caused by modifying CDNC in the different stratocumulus regions is given in Table 1, along with the percentage area of the Earth covered by each region. It is immediately apparent that the RFP produced is of a significant magnitude: modifying all three areas produces an RFP of almost -1 Wm^{-2} , which would offset roughly 35% of the forcing due to current levels of anthropogenic greenhouse gases [IPCC, 2007]. An important difference between the RFP caused by this geoengineering approach and the forcing due to well-mixed greenhouse gases is that the RFP is highly nonuniform, with the majority of the RFP being localized in the modified region. A simple measure of this is the hemispheric RFP shown in Table 1. For the NP case, the ratio between northern and southern hemisphere forcing is a little under 4 to 1, whereas the hemispheric balance is reversed in ALL, with the ratio being approximately 1 to 5 (NH to SH). In the SP and SA cases the RFP is almost totally in the southern hemisphere.

[14] Examination of the global mean RFP values in Table 1 shows that the RFPs are not additive: the sum of the three regions considered separately is -1.31 Wm^{-2} , 35% larger than the RFP produced when all three regions are modified simultaneously. The contribution to the global mean RFP of the modified and unmodified regions in Table 1 shows that the unmodified “rest-of-world” contributes approximately 40% of the RFP in the NP case, almost nothing in SA, and a small counteracting positive RFP in the ALL case. RFP in a given modified area is approximately the same in the ALL simulation as in the corresponding individual-area simulation, indicating that the RFP in a given (modified) stratocumulus region does not depend on whether other stratocumulus regions are being modified. The lack of additivity for RFP may therefore be ascribed to the RFP induced in unmodified areas by the change in climate caused by the geoengineering of the various stratocumulus regions. This also helps explain why the global mean RFPs do not scale with the area of the modified regions (Table 1).

3.2. Climate Sensitivity and Efficacy

[15] Table 2 shows the climate sensitivity (λ , defined as degrees K of near-surface temperature change per Wm^{-2} of RFP) and climate efficacy (λ divided by λ for CO_2 [Hansen *et al.*, 2005]) from the HadGEM2-AML experiments where

each stratocumulus area was modified separately, as well as the ALL case for comparison. The RFP values used to compute these sensitivities are those from the HadGEM2-A simulations presented in Table 1. Previous experiments with this model suggest that climate sensitivity is around $1 \text{ K W}^{-1} \text{ m}^2$ for increases in carbon dioxide [Jones *et al.*, 2007], which is not greatly different to the sensitivity found for the NP or SA cases, i.e. their climate efficacy is close to 100%. However, it is clear that global mean temperature is much more sensitive to perturbations in the South Pacific, which has a climate efficacy more than twice that associated with the other two regions. If only one marine stratocumulus area could be targeted for geoengineering, the larger climate efficacy in the SP case might suggest this as an appropriate candidate. However, it is important to consider the continental and regional scale responses to such localized geoengineering.

3.3. Climate Response

[16] Figure 2 shows the evolution of global mean near-surface air temperature from 2000 to 2060 in the A1B control and ALL geoengineering experiment of the coupled HadGEM2-AO model, in terms of the anomaly with respect to the mean 1860 value. Both A1B and ALL simulations start in the year 2000 at about 0.8 K warmer than the 1860 mean. Thereafter A1B warms by approximately a further 1.7 K by 2060, although there are some periods of little warming (e.g., 2000 to 2010 and 2050 to 2060). Applying the geoengineering modification to all three stratocumulus areas from 2000 in ALL causes the near-surface air temperature to fall rapidly (within 5–10 years) to a value about 0.6 K lower than that in A1B, an offset which is approximately maintained throughout the simulated period. The continuing increase in greenhouse gases eventually causes ALL to warm to the original 2000 level, and then continue to warm up to 2060. However, the geoengineering delays any given amount of warming that would be produced under the A1B scenario by about 25 years. Figure 2 also shows the result of another short experiment where the geoengineering was turned off in 2025. The model warms

Table 2. Climate Sensitivity (λ) and Climate Efficacy (%: λ / λ for CO_2) for Modified Marine Stratocumulus Areas as Determined From HadGEM2-AML Simulations for the Near-Surface Equilibrium Temperature Change (K) and HadGEM2-A Simulations for Radiative Flux Perturbation (Wm^{-2} ; see Table 1)^a

Area Modified	λ ($\text{K W}^{-1} \text{ m}^2$)	Efficacy (%)
NP	0.93 (0.63–1.61)	93
SP	2.27 (1.64–3.63)	227
SA	1.02 (0.63–2.37)	102
ALL	1.83 (1.50–2.35)	183

^aThe range for λ is the 95% confidence interval.

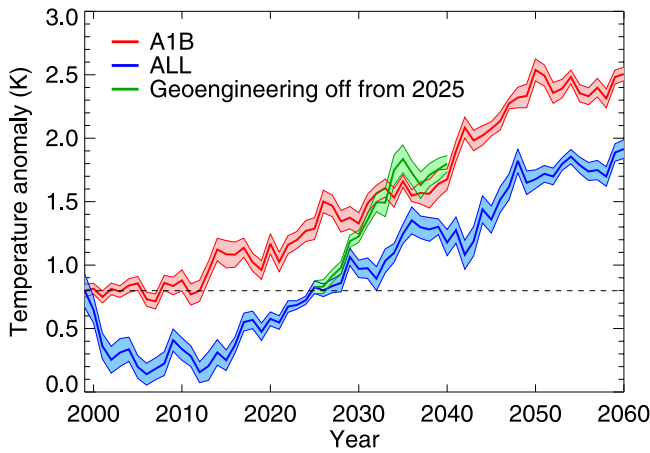


Figure 2. Evolution of near-surface air temperature anomaly (K) with respect to 1860 in HadGEM2-AO. The red line (A1B) indicates the simulation forced by the SRES A1B scenario, and the blue line (ALL) indicates the simulation that also includes the geoengineering of all three stratocumulus areas. The green line indicates a short simulation initialized from ALL at 2025 but with all geoengineering suspended. The envelopes around the lines are a measure of the interannual variability in the simulations, being $\pm 1SD$ based on a detrended nine-point linear fit at each point.

rapidly (by approximately 0.4 K in the first 5 years), and within about 5–10 years the temperature is indistinguishable from that in A1B. This illustrates the fact that if geoengineering is used to “buy us some time”, then an even larger mitigation effort has to be undertaken when geoengineering is stopped to prevent extremely rapid global mean temperature increases, a point already made by Boucher *et al.* [2009].

[17] Figure 3 shows the distribution of near-surface temperature change caused by the geoengineering, calculated as the difference between ALL and A1B aver-

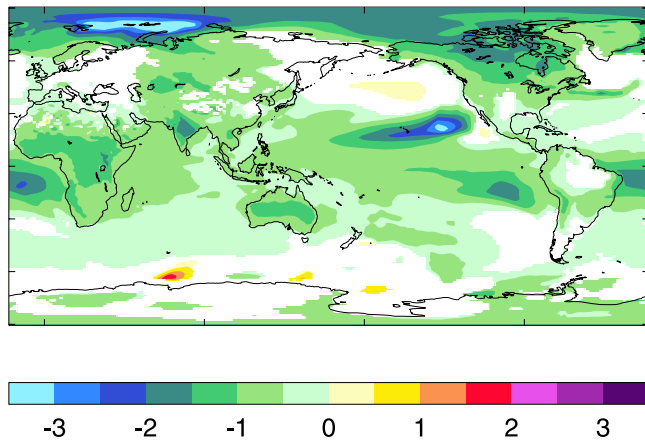


Figure 3. Mean 2030–2059 1.5m temperature change (K) due to geoengineering of the three main marine stratocumulus cloud areas (ALL – A1B). Areas where the difference is not statistically significant at the 5% level are in white.

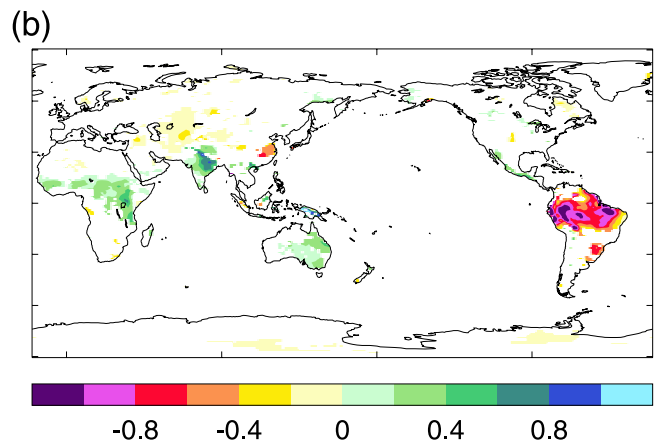
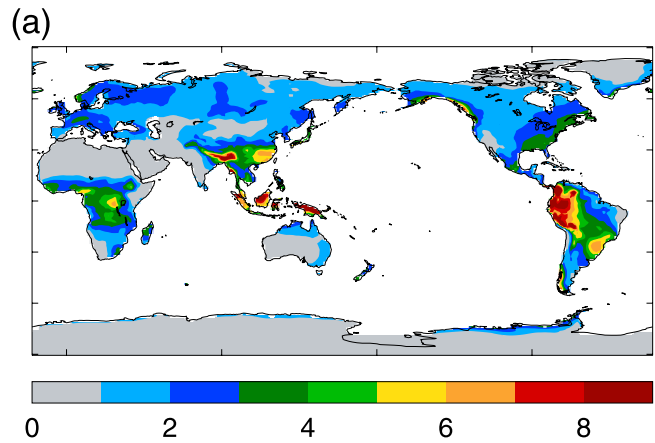


Figure 4. Mean 2030–2059 land precipitation (mm day⁻¹): (a) distribution in A1B; (b) ALL – A1B. Land areas in Figure 4b where the change is not statistically significant at the 5% level are in white.

aged over the 30 years 2030–2059 inclusive. Each 30-year sample was detrended using a linear fit to the annual global means, and then a *t* test applied to the difference at each point. Only those points where the difference is statistically significant at the 5% level are plotted. The global mean cooling of 0.58 K is as expected from Figure 2; however, the distribution of the cooling is quite inhomogeneous. Over the ocean (mean temperature change -0.53 K) there are sizable areas of cooling in the tropics and subtropics associated with the areas of modified cloud, and also a fairly strong cooling response over the Arctic (up to -3 K). On the other hand, large areas of the Southern Ocean are not significantly affected. Over land (mean change -0.70 K), the response is again quite variable. Some areas, such as central Africa, Australia and India, experience over 1 K of cooling. On the other hand, areas such as Europe, the central U.S.A. and large parts of South America show no significant temperature change compared with A1B.

[18] Figure 4a shows the mean distribution of precipitation over land in A1B for the 2030–2059 period, and Figure 4b the change due to the geoengineering. The impact on precipitation over most land areas is insignificant, but there

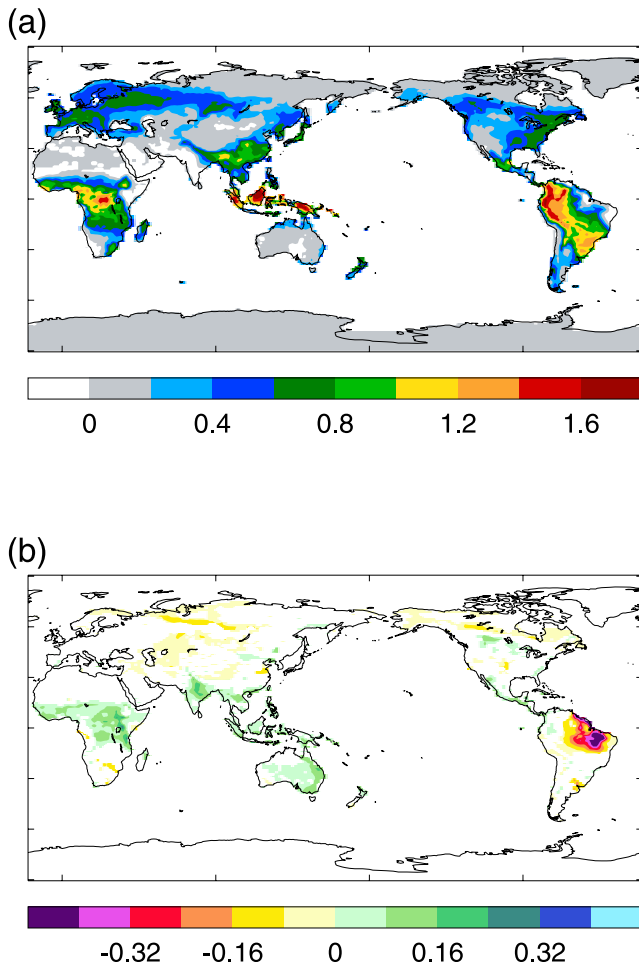


Figure 5. Mean 2030–2059 vegetation net primary productivity ($\text{kg carbon m}^{-2} \text{a}^{-1}$): (a) distribution in A1B; (b) ALL – A1B. Land areas in Figure 5b where the change is not statistically significant at the 5% level are in white.

are obviously important exceptions. Sub-Saharan Africa and eastern Australia show increases of $0.2\text{--}0.6 \text{ mm day}^{-1}$ (10–30%) compared with A1B, which could be beneficial in such low precipitation regions. Larger increases of up to 0.8 mm day^{-1} (>50%) are also present over northern India, another area of low precipitation (Figure 4a). Central Asia shows decreases of around $0.1\text{--}0.2 \text{ mm day}^{-1}$ (~20%), but perhaps the main area for concern is South America, where the Amazonia and Nordeste regions have decreases in precipitation over a large area, with reductions amounting to more than 50% in places.

[19] The distribution of net primary productivity (NPP, a measure of the net carbon uptake by vegetation) and how this is affected by the geoengineering is shown in Figure 5. The distribution of changes in NPP largely corresponds to the changes in precipitation (Figure 4b), showing increases in sub-Saharan Africa, Australia and India, but it also shows a large impact in the north of South America, with reductions corresponding to 50–100% over a considerable area. These results suggest that, although this form of geoengineering might be successful in reducing global mean temperatures, and possibly having other beneficial effects for some

regions, there are also potentially significant consequences for ecosystems in other regions such as the Amazonian rain forest.

[20] To put these changes into context, it is worth knowing what the changes are owing to the A1B scenario alone. Figure 6 shows the mean change in near-surface

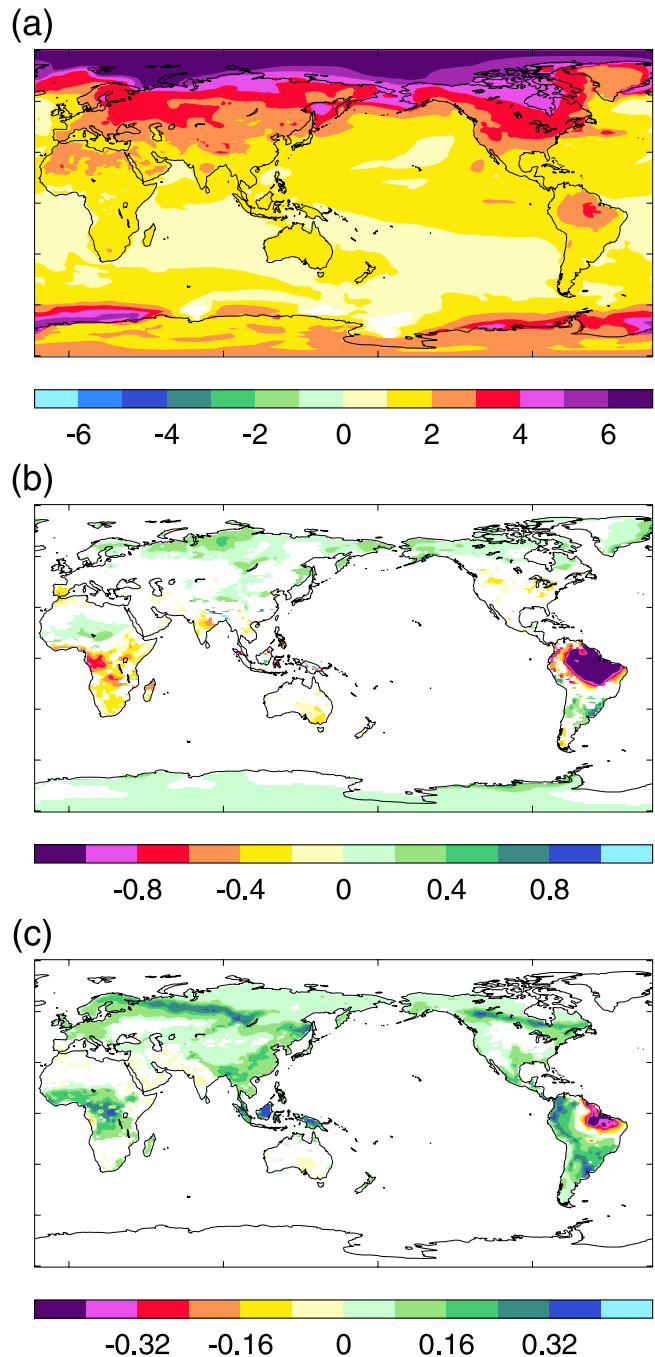


Figure 6. (a) Change in annual mean 1.5 m temperature (K) between 2030–2059 in A1B and 1970–1999 in the historically forced HadGEM2-AO simulation. (b) As in Figure 6a, but for precipitation rate over land (mm day^{-1}). (c) As in Figure 6b, but for NPP ($\text{kg [C] m}^{-2} \text{a}^{-1}$). Areas where the changes are not statistically significant at the 5% level are in white.

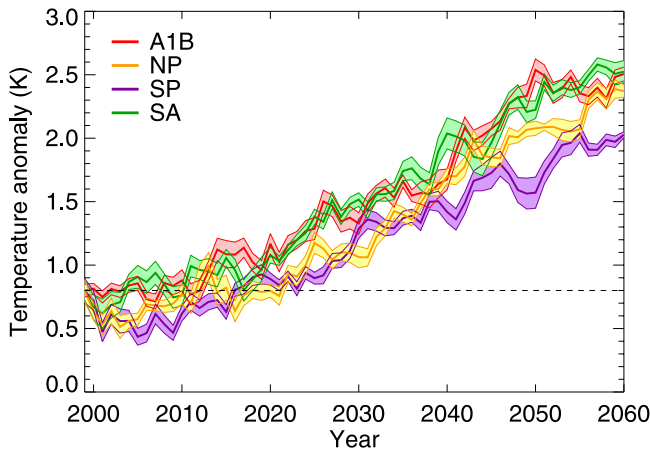


Figure 7. As in Figure 2, but for the SP, NP, and SA HadGEM2-AO experiments compared with the A1B control.

temperature (Figure 6a), land precipitation rate (Figure 6b) and NPP (Figure 6c) between the 2030–2059 period in the A1B scenario and the 1970–1999 period in the historically forced simulation (see section 2). The temperature change shows the typical high-latitude amplification associated with ice albedo feedback, and strong warming of up to 4 K in many northern continental areas. In regions such as central and southern Africa, India and eastern Australia, the unmitigated climate change simulated under A1B causes a decrease in precipitation; the increases in these regions caused by geoengineering (Figure 4b) could therefore be important. The biggest signal is over the north of South America, where there is a large area where precipitation is reduced by over 1 mm day^{-1} , an impact to which geoengineering adds up to a further 1 mm day^{-1} reduction (Figure 4b). The impact of the A1B scenario on NPP in this region is more mixed (Figure 6c), with some increases in the west (presumably due to CO_2 fertilization) but reductions of up to $1 \text{ kg [C] m}^{-2} \text{ a}^{-1}$ in the east, which geoengineering further reduces by half as much again (Figure 5b).

[21] While it is hypothetically feasible to deploy a fleet of cloud seeding vessels to all three of the stratocumulus areas shown in Figure 1, it is informative to investigate the climate response if such vessels were deployed to only one of these areas. The evolution of the global mean near-surface air temperature anomaly from 2000 to 2060 in NP, SP and SA compared with A1B is shown in Figure 7. This shows that the SP simulation is the coolest over most of the simulation period, whereas the SA simulation is largely indistinguishable from the A1B control. Figure 8 shows the distribution of changes in temperature and land precipitation for each case, as well as the sum of the individual responses (Figures 8g and 8h), averaged over the last 30 years of the simulations. These results confirm those from the HadGEM2-AML experiments (section 3.2 and Table 2) suggesting that modifying the South Pacific stratocumulus area has the greatest impact on global temperatures (Figure 8c).

[22] Considering the impact on land areas of modifying the individual stratocumulus regions, Figure 8 again con-

firms that the SP case is the most effective in cooling the land, with North America being cooled by almost 1 K. On the other hand, it also shows that in the SA case many land areas are in fact warmed, the largest impact being a warming of up to 2 K over Amazonia. The biggest impact on land precipitation is also seen in the SA simulation (Figure 8f), with a reduction of over 1 mm day^{-1} over the Amazon region. This reduction due to a cooling in the South Atlantic mirrors a similar feature found in response to a warming of the North Atlantic due to decreasing levels of anthropogenic aerosols reported by Cox *et al.* [2008]. Amazonian rainfall has been shown to be intimately linked to the SST gradient across the Atlantic by shifting the patterns of moisture convergence and trade winds in many global models [e.g., Good *et al.*, 2008; IPCC, 2007]. It appears likely that the decrease in precipitation over the north of South America seen in the ALL simulation (Figure 4b) and the consequent impact on the local ecosystem (Figure 5b) are due to the effect of the modifications to the South Atlantic stratocumulus area. Indeed, the sum of the individual effects shown in Figures 8g and 8h are very similar to the impacts of the ALL simulation (Figures 3 and 4b, respectively), indicating a high degree of additivity of the individual climate responses. Such linearity in the temperature and precipitation responses has been noted in coupled atmosphere-ocean simulations of increases in greenhouse gases and the direct effect of sulfate aerosol, albeit in models with much coarser resolution [Haywood *et al.*, 1997]. This additivity becomes increasingly relevant when considering potential geoengineering solutions as it may be that several geoengineering solutions would need to be deployed to counteract the effects of global warming over centennial timescales.

4. Discussion and Conclusions

[23] We have examined the impact of artificially increasing cloud droplet number concentration in the world's three main regions of persistent marine stratocumulus clouds using both a fully coupled atmosphere/ocean climate model, and also a model where the atmosphere is coupled to a simpler mixed-layer ocean model. It is, however, important to bear in mind that this study only addresses the possible impacts of geoengineering marine clouds as described by Bower *et al.* [2006], Latham *et al.* [2008] and Salter *et al.* [2008], not the mechanism of the proposal itself. Leaving aside technological and operational issues, an important question which needs to be addressed is whether the large-scale injection of sea salt particles into stratocumulus clouds would have the desired effect, i.e. would the cloud properties be modified in the manner suggested by Twomey [1977] and Albrecht [1989]? Studies such as those by Ackerman *et al.* [2004], Xue and Feingold [2006] and Wood [2007] suggest the existence of complex interactions between cloud microphysics, dynamics and the large-scale meteorology, in which the addition of aerosol can either enhance or reduce cloud albedo (see also discussion by Haywood *et al.* [2009]). The conditions under which each response occurs need to be understood before any large-scale modification of clouds is contemplated (as noted by Latham *et al.* [2008]). As well as the detailed work at the cloud scale referred to above, it is also important to

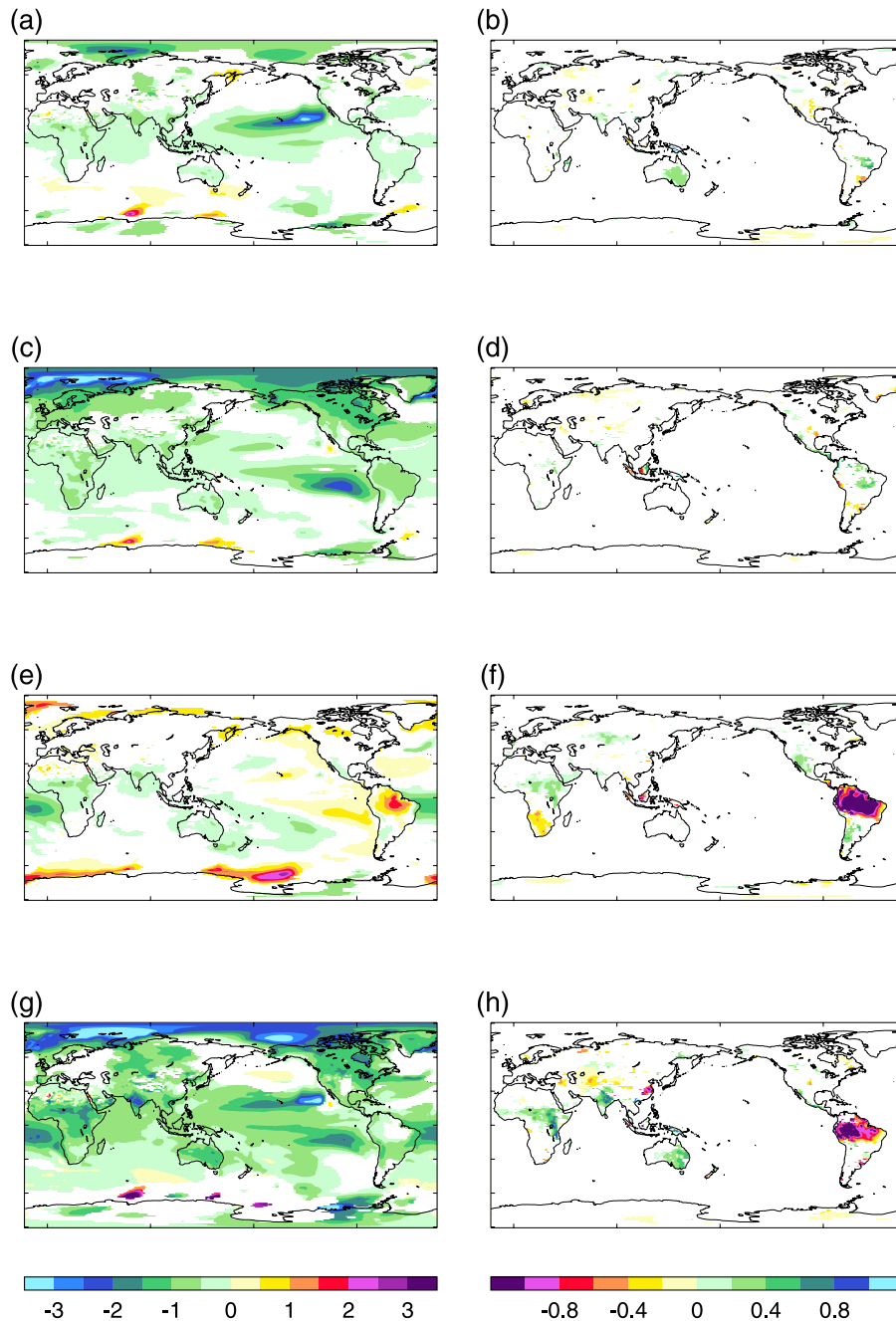


Figure 8. Mean 2030–2059 changes in near-surface air temperature (K, left column) and land precipitation (mm day^{-1} , right column) relative to the A1B control in HadGEM2-AO simulations (a, b) NP, (c, d) SP, and (e, f) SA. (g, h) The sum of the changes due to the individual stratocumulus areas (see Figures 3 and 4b). Changes which are not significant at the 5% level in Figures 8a to 8f are in white. For display purposes, Figures 8g and 8h have had the same significance masks applied to them as used in Figures 3 and 4b respectively.

investigate the climate response to cloud modification in other climate models, to assess the robustness of the responses found in this study.

[24] Our model simulations suggest that, if marine clouds respond in the manner assumed by those proposing such geoengineering, large-scale cloud modification certainly has the potential to reduce global mean temperature by a significant amount. In the coupled-model experiments,

geoengineering all three stratocumulus areas lowered global mean temperature by 0.6 K, which could be interpreted as being equivalent to deferring the expected future global warming by approximately 25 years. However, the studies also show that global mean temperature is not the whole story: there are also regional changes in temperature and precipitation which can be beneficial or detrimental. Whereas there may be potentially beneficial

increases in rainfall in sub-Saharan Africa and Australia, possible negative impacts on the Amazonia and Nordeste regions of South America are indicated, which could further exacerbate global warming as the Amazon rain forest is a major sink for carbon dioxide. Of course, any such potential negative impacts of geoengineering should be considered in terms of the changes that might happen otherwise, but on the other hand this study suggests that it would be wrong to think that geoengineering via cloud modification is a totally reversible (and hence completely benign) process.

[25] Our simulations suggest that if the geoengineering is instantaneously halted, the global mean temperature returns to a nongeoengineered value in around 5–10 years. This result, however, neglects the possible irreversible effect the geoengineering has on the Amazon rain forest and the associated effect on CO₂ levels, and thus on temperature. Such impacts cannot be assessed in this model as CO₂ concentration follows the SRES scenario, rather than being calculated interactively as would be done in a full Earth system model with a carbon cycle. However, it seems plausible that any reduction in carbon sinks caused by geoengineering would reduce its effectiveness in lowering global temperatures, and that if the geoengineering was suddenly terminated, then the reduced carbon sink could mean that temperatures might end up warmer than they would have done otherwise.

[26] The climate impacts described here are, of course, related to the location of the cloud modification; Latham *et al.* [2008], for example, suggest cloud modifications with a rather different distribution. Summing the model response of temperature and precipitation when individual stratocumulus regions are perturbed appears to reasonably represent the temperature and precipitation when all stratocumulus regions are perturbed simultaneously, suggesting an approximate linearity in response for both temperature and precipitation in this model. Our results suggest that any putative attempt at geoengineering via cloud modification should avoid the South Atlantic stratocumulus region as this has little impact on global mean temperature and adversely affects the Amazonian rain forest.

[27] It appears clear from the results of this study that large-scale cloud modification, if successful in increasing cloud albedo to such an extent as to generate a negative global radiative forcing perturbation sufficient to be comparable with the positive forcing due to greenhouse gas increases, is likely to produce changes in climate of its own. Even if the persistent stratocumulus cloud areas studied here were avoided, if the desired negative forcing is to be obtained, then significant cloud modifications will be required somewhere; these will cause their own changes in climate, which should be assessed. Finally, as with all geoengineering, the proposal for large-scale modification of marine clouds also raises ethical and political questions which should be addressed openly before embarking upon any such activity.

[28] **Acknowledgments.** We thank two anonymous reviewers for comments that greatly improved the paper, Sarah Ineson for useful comments on an earlier version of the manuscript, Chris Jones for advice on the land surface scheme, and John Latham and Stephen Salter for useful discussions during the course of writing this manuscript. This work was supported by the Joint DECC, Defra, and MoD Integrated

Climate Programme: DECC/Defra (GA01101) and MoD (CBC/2B/0417_Annex C5).

References

- Ackerman, A. S., M. P. Kirkpatrick, D. E. Stevens, and O. B. Toon (2004), The impact of humidity above stratiform clouds on indirect aerosol climate forcing, *Nature*, *432*, 1014–1017.
- Albrecht, B. A. (1989), Aerosols, cloud microphysics, and fractional cloudiness, *Science*, *245*, 1227–1230.
- Angel, R. (2006), Feasibility of cooling the Earth with a cloud of small spacecraft near the inner Lagrange point (L1), *Proc. Natl. Acad. Sci. U.S.A.*, *103*, 17,184–17,189.
- Bellouin, N., O. Boucher, J. Haywood, C. Johnson, A. Jones, J. Rae, and S. Woodward (2007), Improved representation of aerosols for HadGEM2, *Hadley Cent. Tech. Note 73*, Met Office, Exeter, UK. (Available at <http://www.metoffice.gov.uk/research/hadleycentre/pubs/HCTN/index.html>)
- Boucher, O., J. A. Lowe, and C. D. Jones (2009), Implications of delayed actions in addressing carbon dioxide emission reduction in the context of geo-engineering, *Clim. Change*, *92*, 261–273, doi:10.1007/s10584-008-9489-7.
- Bower, K., T. Choulaton, J. Latham, J. Sahaee, and S. Salter (2006), Computational assessment of a proposed technique for global warming mitigation via albedo-enhancement of marine stratocumulus clouds, *Atmos. Res.*, *82*, 328–336, doi:10.1016/j.atmosres.2005.11.013.
- Boyd, P. W. (2008), Ranking geo-engineering schemes, *Nat. Geosci.*, *1*, 722–724.
- Collins, W. J., et al. (2008), Evaluation of the HadGEM2 model, *Hadley Cent. Tech. Note 74*, Met Office, Exeter, UK. (Available at <http://www.metoffice.gov.uk/research/hadleycentre/pubs/HCTN/index.html>)
- Cox, P. M., P. P. Harris, C. Huntingford, R. A. Betts, M. Collins, C. D. Jones, T. E. Jupp, J. A. Marengo, and C. A. Nobre (2008), Increasing risk of Amazonian drought due to decreasing aerosol pollution, *Nature*, *453*, 212–215, doi:10.1038/nature06960.
- Crutzen, P. J. (2006), Albedo enhancement by stratospheric sulfur injections: A contribution to resolve a policy dilemma?, *Clim. Change*, *77*, 211–220, doi:10.1007/s10584-006-9101-y.
- Essery, R. L. H., M. J. Best, R. A. Betts, P. M. Cox, and C. M. Taylor (2003), Explicit representation of subgrid heterogeneity in a GCM land surface scheme, *J. Hydromet.*, *4*, 530–543.
- Good, P., J. A. Lowe, M. Collins, and W. Moufouma-Okia (2008), An objective tropical Atlantic sea surface temperature gradient index for studies of south Amazon dry-season climate variability and change, *Philos. Trans. R. Soc. B*, *363*, 1761–1766, doi:10.1098/rstb.2007.0024.
- Hansen, J., et al. (2005), Efficacy of climate forcings, *J. Geophys. Res.*, *110*, D18104, doi:10.1029/2005JD005776.
- Haywood, J. M., R. J. Stouffer, R. Wetherald, S. Manabe, and V. Ramaswamy (1997), Transient response of a coupled model to estimated changes in greenhouse gas and sulfate concentrations, *Geophys. Res. Lett.*, *11*, 1335–1338.
- Haywood, J., L. Donner, A. Jones, and J.-C. Golaz (2009), Global indirect radiative forcing caused by aerosols: IPCC (2007) and beyond, in *Clouds in the Perturbed Climate System: Their Relationship to Energy Balance, Atmospheric Dynamics, and Precipitation*, edited by J. Heintzenberg and R. J. Charlson, pp. 451–467, Strüngmann Forum Report, MIT Press, Cambridge.
- IPCC (2007), *Climate Change 2007: The Physical Science Basis. Contribution of Working Group I to the Fourth Assessment Report of the Intergovernmental Panel on Climate Change*, edited by S. Solomon et al., Cambridge Univ. Press, Cambridge, U. K.
- Johns, T. C., et al. (2006), The new Hadley Centre climate model HadGEM1: Evaluation of coupled simulations, *J. Clim.*, *19*, 1327–1353, doi:10.1175/JCLI3712.1.
- Jones, A., D. L. Roberts, M. J. Woodage, and C. E. Johnson (2001), Indirect sulfate aerosol forcing in a climate model with an interactive sulphur cycle, *J. Geophys. Res.*, *106*, 20,293–20,310.
- Jones, A., J. M. Haywood, and O. Boucher (2007), Aerosol forcing, climate response and climate sensitivity in the Hadley Centre climate model, *J. Geophys. Res.*, *112*, D20211, doi:10.1029/2007JD008688.
- Lackner, K. S. (2003), A guide to CO₂ sequestration, *Science*, *300*, 1677–1678, doi:10.1126/science.1079033.
- Latham, J. (1990), Control of global warming?, *Nature*, *347*, 339–340.
- Latham, J. (2002), Amelioration of global warming by controlled enhancement of the albedo and longevity of low-level maritime clouds, *Atmos. Sci. Lett.*, *3*, 52–58, doi:10.1006/asle.2002.0099.
- Latham, J., P. Rasch, C.-C. Chen, L. Kettles, A. Gadian, A. Gettelman, H. Morrison, K. Bower, and T. Choulaton (2008), Global temperature stabilization via controlled albedo enhancement of low-level maritime clouds, *Philos. Trans. R. Soc. A*, *366*, 3969–3987, doi:10.1098/rsta.2008.0137.

- Morton, O. (2007), Is this what it takes to save the world?, *Nature*, 447, 132–136.
- Nakićenović, N., et al. (2000), *IPCC Special Report on Emission Scenarios*, Cambridge Univ. Press, Cambridge, U.K.
- Robock, A. (2008), Whither geoengineering?, *Science*, 320, 1166–1167, doi:10.1126/science.1159280.
- Rossow, W. B., and R. A. Schiffer (1999), Advances in understanding clouds from ISCCP, *Bull. Am. Meteorol. Soc.*, 80, 2261–2287.
- Salter, S., G. Sortino, and J. Latham (2008), Sea-going hardware for the cloud albedo method of reversing global warming, *Philos. Trans. R. Soc. A*, 366, 3989–4006, doi:10.1098/rsta.2008.0136.
- Twomey, S. A. (1977), The influence of pollution on the shortwave albedo of clouds, *J. Atmos. Sci.*, 34, 1149–1152.
- Wigley, T. M. L. (2006), A combined mitigation/geoengineering approach to climate stabilization, *Science*, 314, 452–454, doi:10.1126/science.1131728.
- Wood, R. (2007), Cancellation of aerosol indirect effects in marine stratocumulus through cloud thinning, *J. Atmos. Sci.*, 64, 2657–2669, doi:10.1175/JAS3942.1.
- Xue, H., and G. Feingold (2006), Large-eddy simulations of trade wind cumuli: Investigation of aerosol indirect effects, *J. Atmos. Sci.*, 63, 1605–1622.

O. Boucher, J. Haywood, and A. Jones, Met Office Hadley Centre, FitzRoy Road, Exeter, Devon EX1 3PB, UK. (andy.jones@metoffice.gov.uk)